Adv Polym Sci (2021) 287: 319–342
https://doi.org/10.1007/12_2021_86

Published online: 14 August 2021

Chitosan–Platelet Interactions

C. D. Hoemann and G. -E. Rivard

Contents

Abstract Since chitosan was identified as a hemostatic agent in the 1980s, "chitosan and platelets" has developed into a topic of intense interest. This chapter gives an overview of platelet biogenesis, composition, activation, and mechanisms implicated in chitosan–platelet interactions. Chitosan is a unique acid-soluble cationic glucosamine polysaccharide with tunable molecular weight, glucosamine/N-acetyl glucosamine content, and acetylation pattern. Platelets are small anuclear cells with anionic surfaces that are released to the blood stream by megakaryocytes that reside in bone marrow and the lung. Platelets are stocked with granules that contain a plethora of bioactive wound-healing and procoagulant factors. Upon activation by agonists, or adhesion to von Willebrand factor "strings" under shear stress, platelets aid in fibrin clot formation to seal off a wound and initiate wound repair. Purified platelets rapidly adhere to a variety of solid chitosan and chitin substrates but show inconsistent levels of activation in the absence of calcium. Chitosans with a positive charge state bind to platelets and potentiate alpha granule release in whole blood or recalcified platelet-rich plasma (PRP). Platelet activation kinetics were accelerated by higher chitosan deacetylation levels and molecular weight (95% vs. 80%

C. D. Hoemann (✉)
Department of Bioengineering, George Mason University, Manassas, VA, USA
e-mail: choemann@gmu.edu

G. -E. Rivard
Division of Hematology-Oncology, Hôpital Sainte-Justine, CHU Sainte-Justine, Montreal, QC, Canada

deacetylated, 177 kDa vs. 102 kDa), but mis-timed platelet degranulation prior to thrombin activation led to weaker clot tensile strength. Neutral-soluble chitosans (oligomers, 50% reacetylated chitosans) do not activate platelets and hydrophobic butyryl-chitosan coatings inhibit platelet adhesion. Collective data suggest two mechanisms underlying chitosan–platelet interactions: (1) non-specific electrostatic binding of anionic platelets to positively charged chitosan surfaces, and (2) platelet binding to blood plasma factors adsorbed on chitosan or chitin surfaces. Future directions include deepening our understanding of the molecular basis for thrombocyte–chitosan interactions, and the performance of platelet-activating chitosan formulations in clinically relevant contexts where platelet physiology is altered by medications, trauma, or disease.

Keywords Alpha granule · Calcium · Chitin · Chitosan · Coagulation · Platelets

1 Chitosan Structure and Solubility

According to the Web of Science, the topic of "chitosan and platelets" started gaining attention by the early 2000s, with around 30 papers published per year on this topic. Since then, the number of publications has progressively soared to over 3,200 papers in 2020 alone, with a particular focus in the areas of hemorrhage control and wound repair. To appreciate the molecular and cellular basis of chitosan–platelet interactions, it is first important to understand that chitosan is a family of polymers with distinct chemical structure and physical forms that collectively influence the way the polymer "presents" to platelets.

Chitosan is obtained by chemical N-deacetylation of chitin, a naturally occurring polysaccharide with linearly arranged β-(O)-1-4-linked N-acetyl-D-glucosamine (GlcNAc) residues [1]. The deacetylation step can be simply achieved by autoclaving chitin particles in a 25% w/v sodium hydroxide solution [2, 3]. During this treatment, exposed acetyl groups are stripped from GlcNAc to generate glucosamine (Glc). It was proposed that GlcNAc groups buried in the nucleus of an insoluble chitin particle are protected from deacetylation, giving rise to a "block" acetylation pattern [4]. "Block" acetylation refers to consecutive clusters of GlcNAc residues (i.e., AADA, AAAA, ADAA) interspersed throughout the poly-Glc chain [5, 6]. Repeated autoclaving of chitosan under alkaline conditions can be used to reach >98% DDA, which for all practical purposes is considered fully deacetylated [2]. Because each autoclave cycle produces chain scission, chitosan M_n is inevitably diminished compared to the chitin starting material. Fully deacetylated chitosan can be reacetylated to different % DDA levels using acetic anhydride; this produces chitosans with a random acetylation pattern [2, 7]. All of these production steps create heterogeneities in each chitosan preparation. It is important to recognize that each batch of chitosan has a number-average molecular weight (M_n), degree of deacetylation (DDA), and pattern of acetylation, along with a certain level of

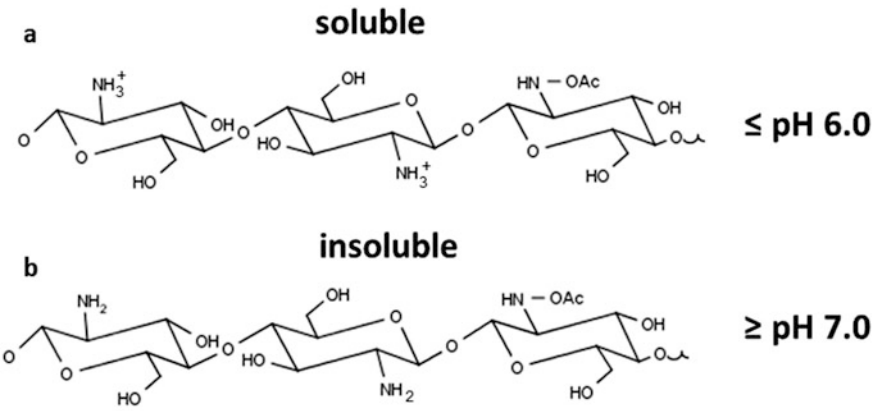

Fig. 1 For chitosan preparations with a molecular weight ≥10 kDa and 60–100% DDA, solution pH controls whether chitosan is (**a**) cationic and soluble or (**b**) neutral and mostly insoluble

polydispersity for each of these characteristics. Each of these structural features can influence the manner in which chitosan interfaces with blood plasma.

As the major structural component of exoskeletons of crustaceans and insects, chitin has evolved to remain firmly insoluble under aqueous conditions. Therefore, chitin particles and scaffolds are by nature insoluble in blood and present slightly hydrophobic poly-GlcNA surfaces to blood components [8, 9]. By contrast, chitosan powders can be dissolved in slightly acidic solutions when at least half of the Glc subunits are protonated (i.e., R-NH_3^+) [10]. In other words, chitosan will only remain soluble at a pH equal to or below the chitosan pK_0. Because all chitosans (60–100% DDA) have a pK_0 6.0–6.5 that is altogether below neutral pH [10, 11], this means that acid-soluble chitosan chains will spontaneously transition into insoluble microparticles upon mixing with neutral pH cell culture medium, blood plasma, or whole blood [12–14] (Fig. 1). When soluble chitosan chains shift to insoluble microparticles in the presence of serum, the microparticles adopt a slight negative zeta potential suggesting that chitosan-anionic serum factor complexes form spontaneously [12, 14]. Solid freeze-dried chitosan scaffolds generated from fully protonated chitosan solutions will spontaneously solubilize in whole blood or platelet-rich plasma and then disperse as microparticles in the coagulum [15–17]. By contrast, chitosan matrices treated with alkaline solutions and/or organic solvents show depressed surface energy and wettability compared to Glc and GlcNAc monomers [18]. Chitosan matrices cured in alkaline conditions have neutral amine groups and present neutral, insoluble surfaces to blood components (Fig. 1b). Chitosan neutral–solubility is enhanced by decreasing molecular weight and by very low deacetylation levels (i.e., 50% DDA) [7, 19]. Small chitosan oligomer chains (≤5 kDa) are fully soluble at neutral pH for all DDA levels [2, 20].

2 Platelets

Platelets are small anuclear disc-shaped cells released by megakaryocytes into the blood circulation [21]. Megakaryocytes are large multinuclear cells derived from a common myeloid progenitor that normally develop and reside in the bone marrow. At full maturity these cells can reach a ploidy up to 64 N [22]. Megakaryocytes are also found in the circulation and are known to populate heart and lung tissues [22–25]. According to the "pulmonary platelet production model", a significant portion of platelets could be produced in the lung [22]. It was suggested that shear forces in the lung vasculature shred apart "proplatelets" released by bone marrow megakaryocytes, while other studies using transgenic mice carrying green fluorescent protein-expressing megakaryocytes revealed that circulating megakaryocytes can lodge in pulmonary vessels and eject platelets directly into the pulmonary vasculature [22, 24, 26]. Circulating platelet levels are under the control of a humoral factor, thrombopoietin (TPO), that is released to the circulation mainly by the liver [22]. Platelet counts in normal adult peripheral blood range from around 115 to 400 $\times$ 10^6/mL. Platelet counts vary with sex and ethnicity, with higher average levels reported for Caucasians compared to Afro-Caribbean and African groups and relatively higher levels in women compared to men [27]. Activated platelets can generate small vesicles called microparticles; microparticles are sub-micron lipid vesicles released from a variety of cell types, including platelets, that wind up in the circulation [28]. Several markers are used to identify and characterize platelets, including membrane receptors P-selectin (CD62P), GPIb/IX/V (CD42), and the GPIIb/IIIa integrin complex (CD41/CD61) (Table 1).

Like red blood cells, platelets have anionic surfaces that repel their spontaneous adhesion to endothelial cells, erythrocytes, and leukocytes whose surfaces are also negatively charged [29]. The platelet glycocalyx is around 20–30 nm thick, an anionic coating of integral membrane glycoproteins, proteoglycans, glycolipids, and factors adsorbed from the blood plasma [30]. Platelets also carry blood group antigens at variable levels on several transmembrane receptors including GPIb and GPIIa and GPIIIa [31]. ABH antigens are fucosylated carbohydrate modifications of blood glycoproteins and glycolipids known to influence the risk of thrombosis in certain disease states [32–34]. In a cohort of 313 Japanese healthy volunteers, platelets showed a "high ABH antigen expressor" phenotype in 7% of the donors [31]. These data highlight donor-specific variations in the platelet glycome. In keeping with other cells, platelets show membrane asymmetry with negatively charged phospholipids hidden in the internal membrane.

Platelets can be activated through distinct mechanisms in static whole blood samples and under shear stress generated by blood flow. During whole blood coagulation initiated in vitro by the extrinsic pathway, thrombin activation initiates platelet activation, and activated platelets help propagate clot formation. Platelet activation is often monitored by the release of alpha granule contents. In a kinetic studies of tissue factor (TF)-induced clotting of recalcified citrated whole blood [35, 36], early thrombin activation (as measured by the appearance of fibrinogen

Table 1 Platelet characteristics

Membrane	**Concentration in plasma (baseline)**	**Concentration in clot serum**
Sphingosine-1 phosphate	190 pmol/mL [78]	480 pmol/mL [78]
Alpha granule factors	**Concentration in plasma (baseline)**	**Concentration in clot serum**
Platelet factor 4 (PF4/CXCL4)[a] (present in alpha granules at about 20,000× higher than plasma concentration)	84 ± 203 IU/mL [79] 12.5 ng/mL [80]	2,345 ± 158 IU/mL [79] 4,400 ng/mL [36]
β-Thromboglobulin (CXCL7; NAP2)[a]	1.75 ± 0.09 ng/mL [81] (a) 2.06 ± 0.06 ng/mL [81] (b)	9.4 ± 3.5 ng/mL [82] 206.9 ± 23.3 ng/mL [83] (a) 182.8 ± 20.1 ng/mL [83] (b) 8.4–24.2 μg/million platelets [37]
Thrombospondin-1 (TSP/THBS1)[b]	0.16 μg/mL [42]	4,900 μg/mL in platelets [42]
Fibrinogen	2–4 mg/mL [84, 85]	140 μg/million platelets [37]
Transforming growth factors β1 (TGF-β1)	0.98 ± 0.26 ng/mL [79]	23.7 ± 4.9 ng/mL [79]
Platelet derived growth factor (PDGF-bb)	0 ng/mL [71]	4.2 ± 0.9 ng/mL [71]
Osteonectin	6.9 ± 1.2 nM [35]	44.6 ± 6.7 nM [35]
Alpha granule transmembrane receptors	**Ligand**	
P-selectin (CD62P) transmembrane receptor	(Inside alpha granules of circulating platelets)	(Exposed on the outer membrane of activated platelet)
GPIIb/IIIa ($\alpha_{IIb}\beta_3$; CD41/CD61; Integrin alpha 2b, ITGA2B)	Fibrin, collagen, vitronectin, fibronectin, thrombospondin [42]	(In alpha granules and on the outer membrane, clusters upon activation)
GPIV (CD36)	Collagen type II, thrombospondin [42]	(Appears on the surface after activation)
Tubular elements	**Plasma concentration**	**Platelet concentration**
von Willebrand factor (vWF)[b]	10 μg/mL in plasma [42] 98 U/dL (type O) [86] 130 U/dL (non-O) [86]	34 μg/mL in platelets [42]
Factor V	6.6 μg/mL in plasma [85]	4.4 ng/million platelets [37]
Dense (delta) granule factors	**Plasma concentration**	**Platelet concentration**
Polyphosphate (i.e., 60 to 100 phosphate units)	N/A	0.92 ± 0.19 nmol/10^8 platelets, intragranular polyP ~130 nM [87]
Calcium	2–2.5 mM [88]	22 ± 2.8 nM in platelet cytosol [87]
ATP, ADP	N/A	23.8, 14.5 nmol/mg platelet protein [37]
Serotonin	N/A	1.5–2.5 nmol/mg platelet protein [37]
P-selectin (CD62P) transmembrane receptor [22] (ligand is PSGL-1)	N/A	(Inside alpha granules of circulating platelets, exposed upon activation)

(continued)

Table 1 (continued)

Outer membrane (resting platelets)	**Ligand** [42]	**Function**
GPIb/IX/V (CD42b/CD42a; GP1BA/GP9/GP5)	Surface-bound vWF, IIa	Adhesion
GPIIb/IIIa ($\alpha_{IIb}\beta_3$; CD41/CD61; ITGA2B or ITGAB/ITGB3)	Fibrin (mainly), collagen, vitronectin, fibronectin, thrombospondin	Aggregation, adhesion
GPIa/GPIIa ($\alpha_2\beta_1$; CD49b/CD29; VLA-2/VLA-4beta; ITGA2/ITGB1)	Collagen type I (mainly); fibronectin	Adhesion
GPIc*/IIa ($\alpha_5\beta_1$; CD49e/CD29; VLA-5; ITGA5)	Fibronectin	Adhesion
GPIc/IIa ($\alpha_6\beta_1$; CD49f/CD29; VLA-6; ITGA6)	Laminin	Adhesion
GPIV (CD36)	Collagen type II, thrombospondin (THBS)	Adhesion, aggregation

N/R not reported, *N/A* not applicable, *IIa* activated thrombin

[35] $N = 18$, from $N = 5$ healthy male and $N = 5$ healthy female human TF-activated recalcified citrated whole blood

[36] non-aspirin-using normal human donors (unspecified number of donors), whole blood +32 μg/mL corn trypsin inhibitor, 40 pmol/L TF, 80 nmol/L phosphatidylserine/phosphatidylcholine (PSPC)

[71] $N = 3$ healthy non-fasting adult female donors, unmodified peripheral blood coagulated for 30 min at 37°C

[78] $N = 6$ healthy adults, venous blood combined with 15% volume ACD (acid citrate-dextrose) 2,000 × *g* 15 min for plasma, or glass tube-induced venous blood clotted at RT for 60 min, 15% ACD added then 2,000 × *g* for 15 min

[79] $N = 12$ healthy participants in their twenties, venous blood poured into 7.5% potassium-EDTA tubes, ice for 1–2 h, or allowed to clot in unspecified tubes for 1–2 h at RT then 1,000 × *g* for 20 min 4°C, re-centrifuge 3,000 × *g* 10 min 4°C

[80] Blood with unspecified anticoagulant from $N = 217$ patients undergoing computed coronary artery angiography

[81] Either (a) $N = 42$ healthy blood donors, 57 ± 1 years old, 22% women, or (b) $N = 45$ patients with critical limb ischemia (CLI), 58 ± 2 years old 18% women or $N = 59$ patients, 57 ± 1 years old 22% women with CLI and type 2 diabetes mellitus; unspecified blood collection method, blood plasma analyzed by ELISA for NAP-2/CXCL7

[82] $N = 7$ orthopedic patients, 3 females, 4 males; mean age = 35 ± 7 years (range = 29–52) without inflammatory diseases who had undergone epidural anesthesia, serum collection method not described

[83] (a) $N = 21$ newly diagnosed patients not yet treated with depression; (b) $N = 25$ age-matched controls

[86] $N = 123$ healthy females, multi-ethnic, citrated platelet-poor plasma

[a]Heparin-binding factor

[b]Expressed in platelets and in endothelial cells

peptide A) occurred at 1 min, platelet activation (measured by release of osteonectin, or platelet factor 4, PF4/CXCL4) occurred at 2–3.5 min, and clotting time (measured by appearance of "clumps" on the sidewalls of the tubes) was observed at 4.7 min [35, 36]. It was estimated that platelets had degranulated around 50% of their alpha granule contents at clotting time [36]. In addition to PF4 and osteonectin, platelet alpha granules release a plethora of bioactive factors: platelet-derived growth factor (PDGF), transforming growth factor β1 (TGF-β1), vascular endothelial growth factor (VEGF), as well as procoagulant factors Factor V (FV), von Willebrand factor (vWF), fibrinogen, and thrombospondin [37]. Activated platelets release other factors from delta granules: adenosine nucleotide diphosphate (ADP) and adenosine triphosphate (ATP), serotonin, calcium, and polyphosphate to name a few (Table 1). Upon activation, platelets change their shape from disc-shaped to spiked spheres, adhere to surfaces, and aggregate. Activated platelets undergo cytosolic calcium spikes, release alpha and delta granule contents, express GPIIb/IIIa on the platelet surface, internalize GPIb, and lose plasma membrane asymmetry which exposes phosphatidylserine on the outer membrane [30]. Phosphatidylserine is a docking site for calcium-dependent binding of activated gla-domain coagulation factor assemblies at the platelet membrane [38]. Generation of thromboxane and thrombin at the platelet surface, along with delta granule release of serotonin and ADP, further promotes platelet activation via platelet surface receptors for each of these agonists [39].

Shear-stress induced platelet activation uses vWF to immobilize platelets at the damaged endothelial cell surface. vWF is a large multimeric glycoprotein that is present in the circulation and stored in platelet alpha granules and in Weibel-Palade bodies of endothelial cells [40]. Upon endothelial damage under blood flow-induced shear stress, vWF "strings" are ejected into the blood stream, forming an attachment site for platelets through GPIb/IX/V receptors [41]. Following platelet activation, the platelet integrin receptor GPIIb/IIIa becomes clustered which enables it to engage with subendothelial collagen fibers, fibrin, vWF and thrombospondin through an RGD sequence [30, 42]. Platelet aggregation during coagulation, and anchoring to fibrin through GPIIb/IIIa receptor interactions, is an essential step in clot retraction and hemostasis [42]. The platelet plug forms a "white thrombus" to seal a damaged blood vessel. Given the essential role for platelets in hemostasis, biomaterial features that stimulate platelet activation are clearly important for applications in hemorrhage control. In other applications involving vascular stents, however, attention has focused on formulating chitosan in a manner to inhibit platelet activation [43].

All of the studies analyzed in this chapter used "normal" or "healthy" donor platelets for chitosan interaction studies, however it is important to keep in mind that platelets from unhealthy individuals could potentially show different responses [33]. Evidence has been accumulating to suggest that platelet composition could be altered by certain disease states. Bone marrow megakaryocytes in normal individuals experience a process termed "emperipolesis" [30, 44]. Emperipolesis is a phenomenon distinct from phagocytosis and involves megakaryocyte ingestion of neutrophils, eosinophils, erythrocytes, and lymphocytes without destruction of ingested cell integrity [30]. This remarkable event was originally suggested to

serve as a mechanism for neutrophil transit from the bone marrow into the vasculature [30]. Emperipolesis is enhanced by endotoxin [45] and in experimental models of idiopathic myelofibrosis [44]. Video-epifluorescence microscopy showed that megakaryocyte uptake of neutrophils resulted in mingling of megakaryocyte-neutrophil membranes and the appearance of neutrophil membranes on circulating platelets [46]. The potential implications of these observations, notably in contexts where emperipolesis involves the trans-cellular transit of inflammatory neutrophils, remain to be identified.

3 Chitosan Interfacing with Blood Plasma

Chitosan membranes, sponges, and solid scaffolds are readily created by processes that neutralize or chemically cross-link glucosamine residues, either before or after electrospinning, surface coating, freeze-drying, precipitation or gelation [1]. These chitosan matrices and substrates are intended to remain intact after immersion in blood or blood plasma [47, 48]. Extensive modification of chitosan amine groups by chemical cross-linking reduces the density of cationic residues available for interaction with anionic blood factors. Furthermore, when solid chitosan matrices are treated with alkaline solutions or organic solvents, they strongly resist dissolving, even when hydrated in acidic aqueous solutions. In hemorrhage control, use of a solid matrix is important because chitosan solutions or powders were found to slow bleeding from capillaries but were unable to arrest arterial bleeding without additional pressure to seal off the broken blood vessel.

In certain wound-repair applications, formulations that generate chitosan microparticles are preferred [16, 49]. For example, when a liquid 80% DDA chitosan isotonic solution pH 4.5 is dispersed into unmodified whole blood and allowed to clot in a glass tube for 30 min at 37°C, the soluble chitosan chains can be observed to precipitate due to the neutral pH environment to form a hybrid biomaterial clot with chitosan microparticles interspersed in the fibrin network (Fig. 2a, b). In another approach, a freeze-dried (FD)-chitosan formulation is prepared with a fully protonated chitosan solution (pH 2.5) under controlled lyophilization conditions (inset, Fig. 2c). When this FD-chitosan scaffold is immersed in recalcified citrated platelet-poor plasma and kept at 37°C for an hour to permit fibrin clot formation (Fig. 2c), the chitosan scaffold rehydrates and disperses to form micro-hydrogel particles within the resulting fibrin clot network (Fig. 2d) [16]. Other FD-chitosan formulations intended for PRP mixing were optimized to contain ~83% DDA ~40 kDa chitosan, lyoprotectant, and calcium chloride. These FD-chitosan cakes solubilize, disperse in platelet-rich plasma (PRP), and form a micro-hydrogel particle scaffold network within the PRP fibrin clot structure [50].

As a cationic polysaccharide, chitosan is capable of forming electrostatic complexes with a variety of blood factors, most of which are anionic. Benesch and Tengvall showed that chitosan-coated surfaces develop a 10 nm thick layer of serum protein that includes serum albumin and complement C3 [51]. It was subsequently

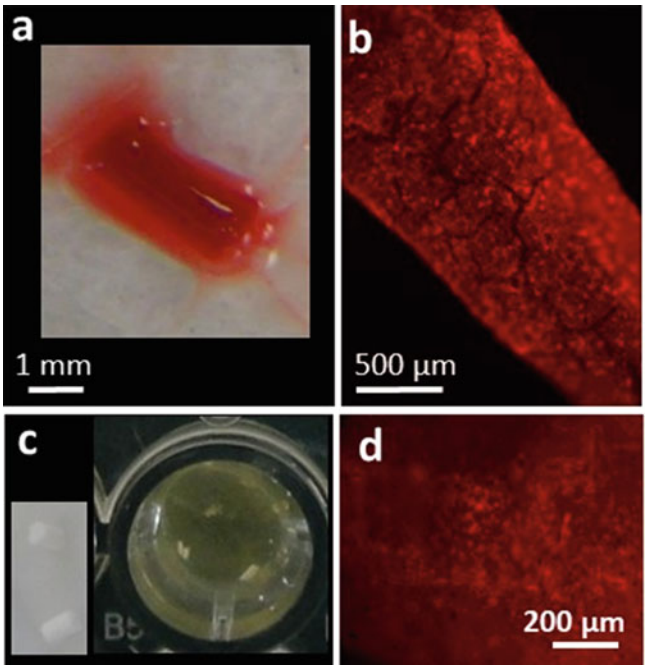

Fig. 2 In certain wound-repair applications, chitosan microparticles are preferred. Two chitosan formulations incorporated with rhodamine isothiocyanate (RITC)-chitosan tracer were used to form hybrid whole blood or recalcified platelet-poor plasma clots and imaged by epifluorescence microscopy. A 1.6% w/v chitosan/100 mM glycerol phosphate solution (RITC-chitosan 80.6% DDA, M_n 46.7 kDa) was mixed at a 1:3 v/v ratio with peripheral whole rabbit blood collected under IRB-approved protocols, and solidified ex vivo in a glass tube to form (**a**) a cylindrical hybrid clot implant with (**b**) RITC-chitosan particles interspersed in the blood clot. (**c**) FD-chitosan (1% w/v chitosan/HCl, pH 2.5, inset) was placed in recalcified citrated human platelet-poor plasma (Precision Biologics, Halifax, Canada) with glass beads to activate coagulation. The FD-chitosan scaffold spontaneously rehydrated and dispersed as micro-hydrogel particles in the fibrin clot (**d**). Panel (**d**) is reprinted from *Materialia,* Vol 9, Hoemann CD et al. Guided bone marrow stimulation for articular cartilage repair through a freeze-dried chitosan microparticle approach, 100609, 2020, with permission from Elsevier

shown that in platelet-poor plasma (PPP), chitosan microparticles form electrostatic complexes with anionic zymogens C3, C5, and Factor B without activating complement [14]. When liquid chitosan is mixed with blood, the chitosan chains form complexes with red blood cells and induce red blood cell agglutination [52]; this bioactivity is attributed to electrostatic binding between chitosan and sialic acid residues on the RBC surface [53]. Platelet activation also activates the complement cascade, therefore chitosan preparations that activate platelets in whole blood or PRP may also drive complement activation indirectly at the platelet surface [14, 54].

The blood stream is maintained in a fluid state partly through its anionic environment. Endothelial cells are coated with a 0.5 mm thick glycocalyx with dense negatively charged heparan sulfate, chondroitin sulfate, and hyaluronan that is shed

into the circulation [55]. The platelet surface carries GPIb receptors with O-linked glycosylations capped with sialic acid, which contribute significantly to the platelet's negatively charged surface [42]. vWF carbohydrate chains are also capped with sialic acid [40, 41]. Desialylation of vWF by neuraminidase leads to its clearance by the liver through the asialoglycoprotein receptor (ASGPR), also called the Ashwell receptor [41, 56]. The Ashwell receptor was also found to be responsible for clearing desialylated platelets that arise during sepsis by the action of bacterial neuraminidase [57]. Fibrinogen is also sialylated [58]. Sialyl groups in fibrinogen were suggested to serve as low-affinity calcium binding sites that favor fibrin self-assembly and branching of fibrin fibers [58]. Because platelet–vWF and platelet–fibrin interactions are mediated through integrin protein receptor interactions (GPIb:vWF; GPIIb/IIIa: fibrin), sialic acid residues in vWF, fibrin, and GPIb are free to interact with other binding partners including cationic glucosamine residues in chitosan. To summarize, the sialic acid modification of glycosylations in many blood factors, blood cell surface receptors, and platelet receptors represents a "sialome" [59] that creates a physicochemical basis for cationic chitosan complex formation. Other anionic blood proteins have a pK_a 6.0 or lower, which enables their binding to chitosan through electrostatic protein–polysaccharide interactions [14].

4 Chitosan–Platelet Interactions

One of the earliest clues that chitosan has procoagulant activity came from experiments by Malette et al., who observed that a porous DeBakey Dacron graft soaked in a 2 mg/mL chitosan solution, but not saline, prevented acute fatal bleed-out when stitched over the excised aorta of heparinized canines [60]. One day later, the chitosan coagulum was found "inside the graft, plugging the interstices" [60]. Klokkevold et al. subsequently observed that lingual hemostasis in rabbits could be accelerated by application of an 80% DDA chitosan solution in acetic acid [61]. In these early reports, the hemostatic mechanism of action was assumed to result from chitosan-induced red blood cell agglutination which creates a "red" thrombus. It was subsequently shown that chitosan-coated microtiter plates, acidic chitosan solutions and chitosan or chitin solid microparticles induce rapid platelet adhesion, aggregation, and elevated surface expression of GPIIb/IIIa in the absence of calcium [62, 63], with one report that chitosan particles could enhance the release of platelet alpha granule contents under calcium-free assay conditions [63] (Table 2). By contrast, neutral-soluble chitosans including chitosan oligomers showed no ability to induce platelet aggregation in vitro and were even slightly anticoagulant [64, 65].

Since these original reports, a variety of hemostatic chitosan devices have been developed, the majority of which are solid matrices, films, coatings, gels, filaments, or sponges that produce hemostasis through mechanisms purporting to involve red blood cell agglutination and/or platelet activation [66, 67]. These devices are intended to promote hemostasis and reside temporarily in the wound. It is important

Table 2 Studies on chitosan–platelet interactions

	Chitin/chitosan	Platelet preparation	Effect of chitin/chitosan
Calcium-free assays			
Chou [62]	Chitosan Mw 50 kDa, >90% DDA (Primex Norway). Dissolve in 2.5% citrate, mix with platelets or use to coat microtiter plates	Rabbit EDTA blood spun at 160 g, 10 min to obtain PRP, platelets washed in calcium-free Tyrode's solution with BSA. 3×10^8 platelets/mL	Rapid platelet adhesion after 5–30 min on chitosan-coated wells. Dose-dependent (10–150 μg/mL chitosan) platelet aggregation and enhanced GPIIb/IIIa expression. When 1 mM external Ca^{2+} is added, chitosan evoked a rise in platelet intracellular Ca^{2+}.
Okamoto [63]	Chitin Mw 300 kDa <10% DDA, 2.8 μm and 6.9 μm particles; chitosan, >80% DDA, Mw 80 kDa, 2.8 μm and 6.2 μm particles (Sunfive Co, Japan). Suspend in PBS pH 7.2, 30 mg/mL	18 mL whole blood from the jugular vein of an unidentified species, mixed with 2 mL 3.8% sodium citrate, 200 g 15 min spin, collect supernatant. Platelets 3×10^5 cells/mL washed in calcium-free Tyrode's buffer, 3×500g 15 min washes. For cytokine release, PRP and chitosan spun at 1,000 g 10 min, then cleared at 10,000 g for 10 min before ELISA	Platelet aggregation ratio (%) was highest at 1 mg/mL with plasma. At 0.3 mg/mL platelet aggregation ratio without or with plasma: chitin 2.8 μm: 14% vs. 19.7%; chitin 6.9 μm: 9.6% vs. 32.3%; chitosan 2.8 μm: 14.2% vs. 15.3%; chitosan 6.2 μm: 14.2% vs. 16.5%. 150% TGF-b1 and 180% PDGF-AB were released by chitosan particles vs. PBS in calcium-free PRP
Thierry [43]	Chitosan (CH) >85% DDA (Sigma), applied layer-by-layer with hyaluronic acid (HA) to NiTi disks or wires	Whole blood from healthy medication-free volunteers collected in ACD, PRP collected at 1800 rpm 15 min, then 2,200 rpm 10 min for PPP supernatant. Platelets labeled with $^{111}InCl_3$ suspended in citrate buffer at 2.5×10^6 platelets/mL. (no Ca added)	50 min incubation with LbL chitosan-HA surfaces gentle shaking, measure adhesion via gamma counter ($^{111}InCl_3$). Observe one million platelets per cm^2 adhered to NiTi, and 600,000 platelets per cm^2 adhered to $HA(CH/HA)_4$
Lin [64]	Chitosan (Koyo Chemical, Japan) nitrite-depolymerized to M_n 0.6 to 2.2 kDa, partly acetylated or fully deacetylated.	Whole venous blood from normal healthy non-aspirin volunteers, 1:9 sodium citrate, $100 \times g$ 15 min RT	Combine 50 μL chitosan +450 μL PRP. Positive control: 20 μM ADP. Oligos had an anticoagulation effect in whole blood. Turbidimetric aggregation measures showed platelet activation

(continued)

Table 2 (continued)

	Chitin/chitosan	Platelet preparation	Effect of chitin/chitosan
	Chitosan at 10% w/v in PBS pH 7.4	(PRP) then 2,000 × *g* 15 min (PPP)	by ADP and not by any chitosan oligos
Fischer [8]	Syvek Patch fibers (50 full acetylated chitin poly-GlcNAc, 3,000 kDa, ≤100 nm fibers) Clo-Sur PAD (87 ± 10% DDA) ChitoSeal (chitosan-coated polyethylene terephthalate, PET) matrix	Fresh human PRP, separated from plasma proteins by gel filtration or centrifugation. 1.5×10^8 platelets/mL in citrated PPP were combined with scaffolds for 3 min, then fixed in formalin, ESEM scanned. (Calcium was only added to PRP without chitin or chitosan)	Syvek fibers: a grape-like platelet-fiber complex with non-discoid morphology was intercalated in the thin chitin fibers Clo-Sur PAD: platelet clusters on the surface, suggested non-specific electrostatic adhesion ChitoSeal: altered platelet morphology, some spreading on the scaffold surface (non-discoid morphology)
Thatte [9]	Poly-N-acetyl glucosamine fibers or chitosan (Marine Polymer Tech., MA, USA)	Fresh human citrated anticoagulated blood diluted 1:20 v/v in HBSS (for surface PS); PRP from sodium citrated blood, purify platelets, adjust to 1.5×10^8 platelets/mL in PPP or Tyrode's buffer, incubate directly with fiber slurry or chitosan solution (polymer 1.1 mg/mL)	Platelets that were washed of plasma proteins associated after 3 min. with poly-GlcNAc fibers that were much thinner in diameter than platelets. Calcium orange dye-loaded platelets incubated with poly-GlcNAc fibers induced intracellular calcium spike in HBSS after 10 min at RT. Citrate blood in HEPES incubated with 0.35 mg/mL poly-GlcNA showed annexin V binding (exposed phosphatidylserine) vs. controls no GlcNAc
Mao [77]	Cellulose films coated with O-butyryl chitosan (OBCS) grafted with p-azidobenzoic acid. Chitosan starting material: 6.7×10^5 g/mol, 90% DDA (Lianyungang Biologicals Inc, China)	PRP of human blood supplied by Blood Center of Nanjing Red Cross, China (addition of calcium not mentioned)	After 1 h of contact, platelets adhered abundantly to cellulose membranes but not to OBCS-grafted cellulose membrane surfaces
Romani [68]	Chitosan 95/50 (HMC +, Germany) dissolved in acetic acid, salts, and sugars, heat-dried and treated in 5% w/v KOH for	Blood from $N = 4$ healthy volunteers with 3.2% citrate, 400 × *g* 10 min, then 200 × *g* 20 min at room temp. Film	Platelets adhered to chitosan films but remained discoid in shape and did not express P-selectin strongly compared to platelets adhered to glass or plastic coverslips

(continued)

Table 2 (continued)

	Chitin/chitosan	Platelet preparation	Effect of chitin/chitosan
	12 h, washed in water until neutral. Sterilize in 75% ethanol, air dry, incubate in PBS	overlaid with PRP for 1 to 2 h at 37°C. Wash with PBS to remove poorly adherent platelets, fix with formalin	
Zhao [75]	Glycidyl methacrylate functionalized quaternized chitosan (shape-memory gel)	PRP from ADC-whole blood spun 115 × *g* 10 min. Drip onto cryogel disks, incubate 37°C 1 h. (no calcium added)	Platelet adhesion and aggregation on the gel surfaces. Propose electrostatic binding of cells, fibronectin, to cationic chitosan quaternary amines
Calcium-containing assays			
Thatte [9]	Poly-N-acetyl glucosamine fibers or chitosan (Marine Polymer Tech., MA, USA). Poly-GlcNAc was used as a suspension in saline. Chitosan solution was created with unspecified pH and osmolality	Fresh human PRP from sodium citrated blood, purify platelets, adjust to 1.5×10^8 platelets/mL in PPP or Tyrode's buffer, add $CaCl_2$, incubate directly with fiber slurry or chitosan solution (polymer 1.1 mg/mL)	In recalcified PRP, poly-GlcNAc fibers incorporated into the fibrin clot (strongest gel with 0.5 mg/mL chitin fibers), observed P-selectin and αIIbβ3 on platelet surfaces. Chitosan solution failed to activate platelets. Diminished fibrin clot formation when platelets were pre-treated with anti-GPIIb/IIIa or anti-CD49f before recalcifying with 0.5 mg/mL poly-GlcNAc (this experiment was missing PRP-only controls no poly-GlcNAc)
Hoemann [71]	Chitosan 81.6% DDA, *M*n 176 kDa, PDI 1.4, <500 EU/g (BioSyntech, Canada) 1.6% w/v chitosan, 100 mM glycerol phosphate pH 6	Healthy human unmodified peripheral whole blood, combine or not with chitosan-GP, 0.5 mL clots incubated in glass tubes at 37°C for up to 4 h	Chitosan-GP/blood clots burst released 2.8 ng/mL PDGF to serum at 30 min post-clotting vs. 4 ng/mL from whole blood and LPS/blood clots
Hattori [65]	Chitosan 85.3% DDA, 888 kDa or 87.6% DDA 247 kDa (Primex, Iceland); chitosan dimers, hexamers (Seikagaku, Japan), 75–85%DDA 50–190 kDa (Sigma) and Primex-derived lower Mw (9–58 kDa) reacetylated chitosans	Male Sprague-Dawley rats, cardiac puncture whole blood in 3.13% sodium citrate, and PRP: 250 g 10 min then 3,000 g, 15 min, recalcify and combine with chitosan solutions in PBS (0.005–0.2% w/v)	Higher erythrocyte sedimentation rates (indirect measure of RBC agglutination) after adding 75–87.6% DDA chitosan, but not 33.6–50.3% DDA chitosan, oligomers, or 275 kDa chitosan. Increased PRP turbidity and disappearance of liquid phase platelets for 75–88% DDA chitosans but not oligomers
Deprés-Tremblay [17]	Chitosan (in-house) 80% DDA, *M*n 38 kDa, dissolved in	$N = 3$ male and $N = 3$ female human donors, PRP	Chitosan inhibited PRP clot retraction; chitosan found to coat platelets by ESEM, suppress

(continued)

Table 2 (continued)

	Chitin/chitosan	Platelet preparation	Effect of chitin/chitosan
	28 mM HCl, Freeze-dried: 1% w/v chitosan, 24.2 mM $CaCl_2$, 1% w/v trehalose	using ACE E-Z PRP system. 160 g, 10 min spin, then 400 g 10 min. 9.3×10^8/mL platelets	platelet aggregation, enhance surface P-selectin, and enhance PDGF and EGF release
Chevrier [15]	Chitosans (in-house), 80–85% DDA; 4–11, 28–56, 79–154 kDa, Freeze-dried: 0.56–1.5% w/v chitosan with lyoprotectant and 42.2 mM $CaCl_2$	Sodium citrate whole blood (12.9 mM citrate) from 5 human donors. 150 g 10 min then 400 g 10 min; 3× enriched for platelets	Mixture of FD-chitosan and PRP accelerated clotting time from 15 min (PRP-only) to ~2.5 min (FD-chitosan/PRP) and created a "paste-like" PRP
Dwivedi [74]	Chitosan (in-house, 80.2% DDA, M_n 36.6 kDa), Freeze-dried with lyoprotectant and $CaCl_2$	9 mL NZW rabbit blood +1 mL 3.8% citrate, 160 g, 10 min, then concentrate platelets at 400 g, 10 min. 3× enriched for platelets	Chitosan-PRP implant showed residency in a microdrilled cartilage lesion in the knee trochlea and after 8 weeks of repair stimulated twofold higher collagen type II content in cartilage repair tissues vs microdrill control defects treated with PRP-alone
Sundaram [69]	Chitosan (Source-Crab, Kyoto chemicals, Japan) Mw 100–150 kDa; 80–85% DDA	Rat whole blood in 3.2% sodium citrate. 500 g, 5 min, then 200 g, 15 min (PRP) or 2,000 g 10 min (PPP), added to 2% chitosan (Cs) with 0.25 potassium aluminum (Al) or 0.25% calcium (Ca) for 5 min at 37°C, rinse to remove unaggregated platelets	LDH (OD490) of adherent platelets used as a measure of platelet aggregation: Greatest OD490 with Cs-Al-Ca. Gel induced RBC agglutination hypothesize electrostatic interactions mediate platelet-chitosan and RBC-Si-chitosan binding. Hemostatic effect in rat liver and femoral artery hemorrhage models (effective for low pressure bleeding contexts)

to note that platelet–chitosan interaction assays have been carried out either in calcium-free (citrated) plasma or buffers, or in the presence of calcium which permits induction of thrombin and subsequent platelet activation by thrombin and a variety of other endogenous agonists.

Depending on the physical form of a chitosan device, platelets may interact with a 2-D or 3-D chitosan surface, filament, microparticle, or soluble chitosan chain. The Syvek patch is composed of solid chitin fibers, whereas Clo-sur PAD and ChitoSeal are solid patches containing chitosan. Platelets were found to adhere to all three

scaffolds, with evidence of induced P-selectin and GPIIb/IIIa expression when calcium-activated PRP was combined with a slurry of GlcNAc fibers [8, 9]. Platelets also adhered and aggregated on the smoother surfaces of chitosan-based Clo-sur PAD after 3 min, but were mainly observed adhering to exposed polyethylene terephthalate (PET) polymer surfaces on ChitoSeal [8]. In a swine splenic capsular stripping hemorrhage model, the Syvek patch produced hemostasis after three compressions compared to 8–10 for gauze, Clo-sur PAD or ChitoSeal [8]. In another study analyzing platelet adhesion under calcium-free conditions by Romani et al., alkaline-cured chitosan films supported platelet adhesion but the platelets remained discoid in shape and scarcely expressed P-selectin, while platelets adhering to glass coverslips became spiked and had strong P-selectin expression [68]. In another study by Sundaram et al., a chitosan-aluminum sulfate-calcium hydrogel was created that induced platelet aggregation, RBC agglutination, and more rapid hemostasis in rat hemorrhage models [69] (Table 2).

For wound-healing applications, some chitosan devices have been formulated to intermingle as micron-sized hydrogel particles within blood or platelet-rich plasma clots. As mentioned above, viscous isotonic chitosan solutions can be mixed with unmodified whole blood and allowed to coagulate to form a hybrid blood clot [53]. Mixture of liquid chitosan-glycerol phosphate solutions into whole blood produces a hybrid clot that, like whole blood, solidifies through the common pathway of the coagulation enzyme cascade [70]. In thromboelastography (TEG) tests, hybrid clots containing 80% DDA chitosan showed thrombin activation starting at 20 min, followed by burst platelet activation around 30 min marked by release of PF4/CXCL4 and PDGF-ββ into the serum [70, 71]. The dispersion of 80% DDA chitosan microparticles in the hybrid clot implant was found to inhibit clot retraction, protect the clot from lysis by plasmin, promote longer in situ clot residency, attract neutrophils and M2 macrophages, and exert favorable effects on osteochondral wound repair [72, 73].

Here we report the effect of chitosan structure on platelet activation in whole blood, using a library of chitosans with 80% or 95% DDA and low (80L, 95L) or high viscosity (80M, 95M) [12]. Each chitosan was prepared as a 1.6% w/v solution in 100 mM glycerol phosphate (pH 6.0) and mixed or not with unmodified human whole blood from 4 healthy donors. Samples were either harvested immediately, submitted to a TEG assay at 37°C for 160 min to assess clotting time and clot tensile strength, or cultured at 37°C for 240 min in glass tubes. As a model system, blood clots held at body temperature have the potential to reflect platelet responses that could occur in a blood clot device in vivo. At different time points ($t = 0$, 160 or 240 min), using previously described methods [70], samples were vortexed in ice cold quench buffer, centrifuged, and the supernatant analyzed by Western blotting for PF4, or ELISA assay for thrombin-antithrombin (TAT) complex (Dade) (Fig. 3).

95M chitosan (high DDA and medium viscosity) had a unique effect on inducing instant release of PF4 at $t = 0$ in all 4 donors (lane 4, Fig. 3a), prior to thrombin activation (Fig. 3b). 95M also created a rapid increase in blood viscosity that was "read" by the TEG instrument as a more rapid "clotting time" compared to all other

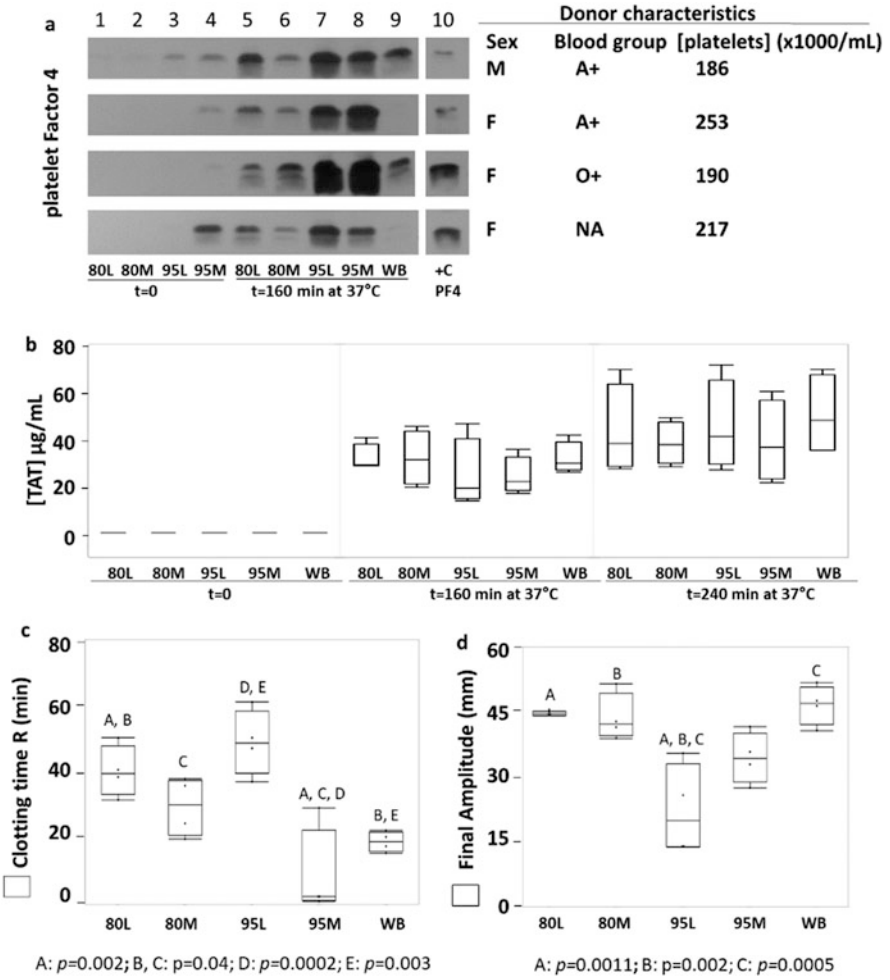

Fig. 3 Chitosan structure influenced the timing of platelet degranulation, clotting time and clot tensile strength in unmodified whole human blood. Under IRB-approved protocols, whole blood from 4 healthy human donors was mixed at 3:1 ratio with chitosan-glycerol phosphate solutions (80L, 80M, 95L, 95M) to evaluate (**a**) PF4 levels in plasma or serum using equal amounts of protein per lane and purified PF4 as a control, (**b**) TAT complex formation in plasma or serum, (**c**) clotting time (R, min), and (**d**) clot amplitude at 160 min (A, mm) by TEG assay. Chitosan (DDA and M_n) were 80L (80.2%, 108 kDa), 80M (80.6%, 144 kDa), 95L (94.6%, 102 kDa), 95M (94.6%, 177 kDa) [12]. Graphs show the median, 50% inter-quartile range, min-max, and differences due to condition were evaluated by Least Squares Means Differences with Tukey HSD post-hoc (JMP Pro 14.1.0, SAS). *R* clotting time, *NA* not available, *WB* whole blood, *TAT* thrombin-antithrombin, *PF4* platelet factor 4, *M* male, *F* female

chitosans (Fig. 3c). All chitosan-GP/blood mixtures coagulated and showed robust TAT generation at 160 and 240 min (Fig. 3b). However lower molecular weight chitosans (80L, 95L) delayed clotting time (Fig. 3c), and 95L induced a weaker clot

tensile strength compared to other clot samples (Fig. 3d). After 240 min at 37°C, PF4 was detected in serum of all chitosan-GP/blood samples, with the highest PF4 levels in 95L and 95M serum (lanes 5–8, Fig. 3a).

In this experiment, unmodified whole blood had a median 18.9 min clotting time, 47.0 mm clot tensile strength (Fig. 3c, d), robust TAT levels after 240 min (48 μg/mL, Fig. 3b), and variable serum PF4 levels at 160 min (lane 9, Fig. 3a). Donor-to-donor differences in serum PF4 levels at 160 min were not explained by selected donor characteristics (Fig. 3a). These results are consistent with previous analyses of healthy donor whole blood: 15.3 ± 4.8 min clotting time, 55.2 ± 5.7 mm maximal amplitude, ~37 μg/mL TAT, and burst appearance of PF4 at 30 min that decayed over time [70]. Altogether, these data suggested that highly deacetylated cationic chitosan chains formed complexes with platelets and red blood cells and may have formed inhibitory complexes with factors that degrade PF4. These results also suggested that platelet responses to chitosan can be influenced by the chitosan charge state at the time of platelet contact and that cationic chitosan is an effective platelet-activating biomaterial. However strong chitosan platelet–interactions by 95L were accompanied by prolonged clotting time and weaker clot tensile strength, which are considered anti-hemostatic effects.

Many experiments analyzing chitosan–platelet interactions are carried out with PRP (Table 2). PRP is generated from citrated whole blood by sequential centrifugation (200 g 15 min to pellet RBC and WBC, then 1,300 g 10 min to pellet platelets). Citrate chelates all plasma calcium and serves as an anticoagulant because calcium is required for propagation of the coagulation factor enzyme cascade leading to thrombin activation and conversion of fibrinogen to fibrin. Therefore, PRP must be recalcified to produce a PRP fibrin clot. Mixture of freeze-dried chitosan containing calcium chloride with PRP resulted in solubilization of chitosan in plasma followed by chitosan coating of platelet surfaces, hybrid chitosan/PRP clot formation, inhibition of PRP fibrin clot retraction, enhanced release of PDGF-ββ, and higher P-selectin expression [15, 17, 50]. Unlike other chitosan–platelet interactions, this FD-chitosan preparation enhanced platelet degranulation while inhibiting platelet aggregation [17]. It was suggested that chitosan inhibited clot retraction in these PRP samples by coating the platelet surfaces and preventing their aggregation [17]. FD-chitosan/PRP showed beneficial biological effects compared to PRP-alone in promoting chondrogenesis in a rabbit cartilage repair model, with greater repair tissue collagen type II content compared to PRP-alone [74]. In other applications, a shape-memory gel containing glycidyl methacrylate functionalized quaternized chitosan, with a permanent positive charge, showed platelet adhesion and aggregation on the surfaces after incubating with citrated PRP for 1 h at 37°C [75]. In the latter study, calcium was not added to the PRP preparation, suggesting the interaction was based on electrostatic interactions between anionic platelet surfaces and the cationic quaternized chitosan.

Platelet adhesion is an undesired event for vascular stents. Coating of a NiTi surface with layer-by-layer (LbL) hyaluronic acid (HA) and chitosan, with the final layer being HA was shown to reduce platelet adhesion from 1 million to 0.6 million platelets/cm^2 [43]. The persistent platelet interactions with LbL-HA(Chitosan/HA)$_4$

could be due to an irregular surface coating by HA after only 4 bi-layers that left exposed chitosan, as another study suggested that at least 6 alternating layers are needed to create a uniform anionic polyelectrolyte surface [76]. By contrast, surface coatings created with chitosans derivatized with hydrophobic butyryl functional groups and covalently attached to cellulose were shown to repel platelets and inhibit platelet adhesion and activation [77] (Table 2).

5 Conclusions and Future Perspectives

To summarize, current data suggest that chitosan–platelet interactions occur through two mechanisms. By one mechanism, electrostatic binding between the anionic platelet surface and cationic chitosan poly-glucosamine residues produces platelet adhesion that can trigger a rise in intracellular calcium, degranulation, and appearance of integrin and P-selectin receptors at the platelet surface [8, 62, 69, 75] (Fig. 4). Platelet GPIb is heavily sialylated and could potentially mediate this interaction. Neutral chitosan and chitin have little capacity to induce these responses. Although most solid matrices used as hemostatic devices have no charge (poly-GlcNAc), or are neutralized during manufacturing, recent advances have created quaternary chitosans with a permanent cationic charge state [75], which enables mechanism 1. By a second mechanism that is likely to take place in blood or PRP, abundant anionic blood plasma proteins (i.e., sialyl-fibrinogen, fibronectin, sialyl-vWF, albumin) rapidly bind to chitosan surfaces. Blood proteins are also expected to deposit on chitin surfaces. Deposition of these matricellular factors, also called "biofouling" presents a surface that permits platelet adhesion, activation, GPIIb/IIIa clustering,

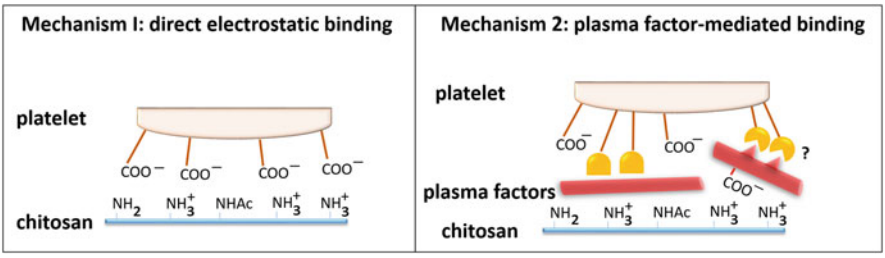

Fig. 4 Two mechanisms are proposed to explain chitosan–platelet interactions. By mechanism 1, platelet anionic surfaces form non-specific electrostatic interactions with chitosan amine groups that are initially protonated at the time of contact with whole blood or PRP. Because anionic blood proteins (including sialylated proteins such as fibrinogen) vastly outnumber platelets, most platelet interactions in PRP or blood likely occur through mechanism 2. In mechanism 2, soluble factors in blood plasma form complexes with chitosan or chitin and display binding sites, some of which may be specific high-affinity interactions via platelet surface receptors (i.e., integrin GPIIb/IIIa, GPIV, GPIc/IIa, GPIc*/IIa, GPIb/IX/V). The schematics show only one side of the platelet surface and are not to scale: platelets are on average 2 μm in diameter [30]. Note that chitosan microparticles that form in blood plasma can have a similar or smaller size compared to platelets, or a much larger size when chitosan aggregates are formed [12]

and the potential for specific receptor–ligand interactions between platelet integrins and RGD motifs in the protein coating (Fig. 4). Evidence for this second mechanism comes from slightly greater platelet aggregation induced by 2.8–6.9 μm chitin or chitosan particles in the presence of plasma proteins compared to platelets washed to remove plasma proteins [63]. Future directions on this topic will benefit from further elucidation of molecular mechanisms involved in chitosan-platelet adhesion and experiments that show the biological relevance of these interactions in whole blood where erythrocytes vastly outnumber platelets. More information is also needed on the performance of platelet-activating chitosan devices in clinical contexts, most notably where platelet physiology is altered by medications, trauma, or disease state.

Acknowledgements We thank Catherine Marchand for PF4 and TAT analyses and J. Guzmán-Morales and J. Sun for hybrid blood clot images. Funding: Canadian Institutes of Health Research Operating grant; Prima-Ortho grant; George Mason University start-up funds.

Competing interest statement: C. Hoemann is a shareholder and on the Scientific Advisory Board of Ortho RTi.

References

1. Khor E, Lim LY (2003) Implantable applications of chitin and chitosan. Biomaterials 24:2339–2349. https://doi.org/10.1016/S0142-9612(03)00026-7
2. Fong D, Grégoire-Gélinas P, Cheng AP, Mezheritsky T, Lavertu M, Sato S, Hoemann CD (2017) Lysosomal rupture induced by structurally distinct chitosans either promotes a type 1 IFN response or activates the inflammasome in macrophages. Biomaterials 129:127–138. https://doi.org/10.1016/j.biomaterials.2017.03.022
3. Chang KLB, Tsai G, Lee J, Fu W-R (1997) Heterogeneous N-deacetylation of chitin in alkaline solution. Carbohydr Res 303:327–332. https://doi.org/10.1016/S0008-6215(97)00179-1
4. Lamarque G, Viton C, Domard A (2004) Comparative study of the first heterogeneous deacetylation of α- and β-chitins in a multistep process. Biomacromolecules 5:992–1001. https://doi.org/10.1021/bm034498j
5. Vårum KM, Anthonsen MW, Grasdalen H, Smidsrød O (1991) 13C-N.m.r. studies of the acetylation sequences in partially N-deacetylated chitins (chitosans). Carbohydr Res 217:19–27. https://doi.org/10.1016/0008-6215(91)84113-S
6. Sashiwa H, Saimoto H, Shigemasa Y, Ogawa R, Tokura S (1991) Distribution of the acetamide group in partially deacetylated chitins. Carbohydr Polym 16:291–296. https://doi.org/10.1016/0144-8617(91)90114-R
7. Kubota N, Tatsumoto N, Sano T, Toya K (2000) A simple preparation of half N-acetylated chitosan highly soluble in water and aqueous organic solvents. Carbohydr Res 324:268–274. https://doi.org/10.1016/s0008-6215(99)00263-3
8. Fischer TH, Connolly R, Thatte HS, Schwaitzberg SS (2004) Comparison of structural and hemostatic properties of the poly-N-acetyl glucosamine Syvek Patch with products containing chitosan. Microsc Res Tech 63:168–174. https://doi.org/10.1002/jemt.20017
9. Thatte HS, Zagarins S, Khuri SF, Fischer TH (2004) Mechanisms of poly-N-acetyl glucosamine polymer-mediated hemostasis: platelet interactions. J Trauma 57:S13–S21. https://doi.org/10.1097/01.TA.0000136743.12440.89
10. Rinaudo M, Pavlov G, Desbrières J (1999) Influence of acetic acid concentration on the solubilization of chitosan. Polymer 40:7029–7032. https://doi.org/10.1016/S0032-3861(99)00056-7

11. Filion D, Lavertu M, Buschmann MD (2007) Ionization and solubility of chitosan solutions related to thermosensitive chitosan/glycerol-phosphate systems. Biomacromolecules 8:3224–3234. https://doi.org/10.1021/bm700520m
12. Hoemann CD, Guzmán-Morales J, Tran-Khanh N, Lavallée G, Jolicoeur M, Lavertu M (2013) Chitosan rate of uptake in HEK293 cells is influenced by soluble versus microparticle state and enhanced by serum-induced cell metabolism and lactate-based media acidification. Molecules 18:1015–1035. https://doi.org/10.3390/molecules18011015
13. Hoemann CD, Hurtig M, Rossomacha E, Sun J, Chevrier A, Shive MS, Buschmann MD (2005) Chitosan-glycerol phosphate/blood implants improve hyaline cartilage repair in ovine microfracture defects. J Bone Joint Surg 87:2671–2686. https://doi.org/10.2106/JBJS.D.02536
14. Marchand C, Bachand J, Périnêt J, Baraghis E, Lamarre M, Rivard GE, De Crescenzo G, Hoemann CD (2009) C3, C5, and factor B bind to chitosan without complement activation. J Biomed Mater Res 9999A. https://doi.org/10.1002/jbm.a.32638
15. Chevrier A, Darras V, Picard G, Nelea M, Veilleux D, Lavertu M, Hoemann CD, Buschman MD (2018) Injectable chitosan-platelet-rich plasma implants to promote tissue regeneration: *in vitro* properties, *in vivo* residence, degradation, cell recruitment and vascularization: chitosan-PRP injectable implants for tissue repair. J Tissue Eng Regen Med 12:217–228. https://doi.org/10.1002/term.2403
16. Hoemann CD, Guzmán-Morales J, Picard G, Chen G, Veilleux D, Chevrier A, Sim S, Garon M, Quenneville E, Lafantaisie-Favreau C-H, Buschmann MD, Hurtig MB (2020) Guided bone marrow stimulation for articular cartilage repair through a freeze-dried chitosan microparticle approach. Materialia 9:100609. https://doi.org/10.1016/j.mtla.2020.100609
17. Deprés-Tremblay G, Chevrier A, Tran-Khanh N, Nelea M, Buschmann MD (2017) Chitosan inhibits platelet-mediated clot retraction, increases platelet-derived growth factor release, and increases residence time and bioactivity of platelet-rich plasma *in vivo*. Biomed Mater 13:015005. https://doi.org/10.1088/1748-605X/aa8469
18. Cunha AG, Fernandes SCM, Freire CSR, Silvestre AJD, Neto CP, Gandini A (2008) What is the real value of Chitosan's surface energy? Biomacromolecules 9:610–614. https://doi.org/10.1021/bm701199g
19. Onishi H, Machida Y (1999) Biodegradation and distribution of water-soluble chitosan in mice. Biomaterials 20:175–182. https://doi.org/10.1016/S0142-9612(98)00159-8
20. Aam BB, Heggset EB, Norberg AL, Sørlie M, Vårum KM, Eijsink VGH (2010) Production of Chitooligosaccharides and their potential applications in medicine. Mar Drugs 8:1482–1517. https://doi.org/10.3390/md8051482
21. George JN, Colman RW (2001) Platelets. In: Hemostasis & thrombosis: basic principles & clinical practice. 4th edn. Lippincott Williams & Wilkins, Baltimore, pp 381–386
22. Kuter DJ (2001) Megakaryopoiesis and thrombpoiesis. In: Williams hematology. 6th edn. McGraw-Hill, New York, pp 1339–1355
23. Cunin P, Nigrovic PA (2019) Megakaryocytes as immune cells. J Leukoc Biol 105:1111–1121. https://doi.org/10.1002/JLB.MR0718-261RR
24. Lefrancais E, Ortiz-Munoz G, Caudrillier A, Mallavia B, Liu F, Sayah D, Thornton E, Headley M, David T, Coughlin S, Krummel M, Leavitt A, Passegué E, Looney M (2017) The lung is a site of platelet biogenesis and a reservoir for hematopoietic progenitors. Nature 544. https://doi.org/10.1038/nature21706
25. Rapkiewicz AV, Mai X, Carsons SE, Pittaluga S, Kleiner DE, Berger JS, Thomas S, Adler NM, Charytan DM, Gasmi B, Hochman JS, Reynolds HR (2020) Megakaryocytes and platelet-fibrin thrombi characterize multi-organ thrombosis at autopsy in COVID-19: a case series. EClinicalMedicine 24:100434. https://doi.org/10.1016/j.eclinm.2020.100434
26. Lefrançais E, Looney MR (2019) Platelet biogenesis in the lung circulation. Physiology (Bethesda) 34:392–401. https://doi.org/10.1152/physiol.00017.2019
27. Ryan DH (2001) Examination of the blood. In: Williams hematology. 6th edn. McGraw-Hill, New York, pp 9–16

28. Owens AP, Mackman N (2011) Microparticles in hemostasis and thrombosis. Circ Res 108:1284–1297. https://doi.org/10.1161/CIRCRESAHA.110.233056
29. Alphonsus CS, Rodseth RN (2014) The endothelial glycocalyx: a review of the vascular barrier. Anaesthesia 69:777–784. https://doi.org/10.1111/anae.12661
30. Cramer EM (2001) Platelets and megakaryocytes: analtomy and structural organization. In: Hemostasis & thrombosis: basic principles & clinical practice. 4th edn. Lippincott Williams & Wilkins, Baltimore, pp 411–428
31. Ogasawara K, Ueki J, Takenaka M, Furihata K (1993) Study on the expression of ABH antigens on platelets. Blood 82:993–999. https://doi.org/10.1182/blood.V82.3.993.993
32. Cooling L (2015) Blood groups in infection and host susceptibility | clinical microbiology reviews. Clin Microbiol Rev 28:801–870. https://doi.org/10.1128/CMR.00109-14
33. Verhoef PA, Kannan S, Sturgill JL, Tucker EW, Morris PE, Miller AC, Sexton TR, Koyner JL, Hejal R, Brakenridge SC, Moldawer LL, Hotchkiss RS, Blood TM, Mazer MB, Bolesta S, Alexander SA, Armaignac DL, Shein SL, Jones C, Hoemann CD, Doctor A, Friess SH, Parker RI, Rotta AT, Remy KE, for the B. and T.S.C. of the R.S. for the S. of C.C (2021) Medicine, severe acute respiratory syndrome–associated coronavirus 2 infection and organ dysfunction in the ICU: opportunities for translational research. Critic Care Explor 3:e0374. https://doi.org/10.1097/CCE.0000000000000374
34. Stowell SR, Stowell CP (2019) Biologic roles of the ABH and Lewis histo-blood group antigens part II: thrombosis, cardiovascular disease and metabolism. Vox Sang 114:535–552. https://doi.org/10.1111/vox.12786
35. Brummel KE, Paradis SG, Butenas S, Mann KG (2002) Thrombin functions during tissue factor–induced blood coagulation. Blood 100:148–152. https://doi.org/10.1182/blood.V100.1.148
36. Rand MD, Lock JB, van't Veer C, Gaffney DP, Mann KG (1996) Blood clotting in minimally altered whole blood. Blood 88:3432–3445
37. Fukami MH, Holmsen H, Kowalska A, Niewiarowski S (2001) Platelet secretion. In: Hemostasis & thrombosis: basic principles and clinical practice. 4th edn. Lippincott Williams & Wilkins, Baltimore, pp 561–573
38. Contreras-García A, D'Elía NL, Desgagné M, Lafantaisie-Favreau C-H, Rivard G-E, Ruiz J-C, Wertheimer MR, Messina P, Hoemann CD (2019) Synthetic anionic surfaces can replace microparticles in stimulating burst coagulation of blood plasma. Colloids Surf B Biointerfaces 175:596–605. https://doi.org/10.1016/j.colsurfb.2018.11.066
39. Rivera J, Lozano ML, Navarro-Nunez L, Vicente V (2009) Platelet receptors and signaling in the dynamics of thrombus formation. Haematologica 94:700–711. https://doi.org/10.3324/haematol.2008.003178
40. Lenting PJ, Christophe OD, Denis CV (2015) von Willebrand factor biosynthesis, secretion, and clearance: connecting the far ends. Blood 125:2019–2028. https://doi.org/10.1182/blood-2014-06-528406
41. Bryckaert M, Rosa J-P, Denis CV, Lenting PJ (2015) Of von Willebrand factor and platelets. Cell Mol Life Sci 72:307–326. https://doi.org/10.1007/s00018-014-1743-8
42. Parise LV, Smyth SS, Coller BS (2001) Platelet morphology, biochemistry, and function. In: Williams hematology. 6th edn. McGraw-Hill, New York, pp 1357–1408
43. Thierry B, Winnik FM, Merhi Y, Silver J, Tabrizian M (2003) Bioactive coatings of endovascular stents based on polyelectrolyte multilayers. Biomacromolecules 4:1564–1571. https://doi.org/10.1021/bm0341834
44. Schmitt A, Jouault H, Guichard J, Wendling F, Drouin A, Cramer EM (2000) Pathologic interaction between megakaryocytes and polymorphonuclear leukocytes in myelofibrosis. Blood 96:1342–1347. https://doi.org/10.1182/blood.V96.4.1342
45. Tanaka M, Aze Y, Shinomiya K, Fujita T (1996) Morphological observations of megakaryocytic emperipolesis in the bone marrow of rats treated with lipopolysaccharide. J Vet Med Sci 58:663–667. https://doi.org/10.1292/jvms.58.663

46. Cunin P, Bouslama R, Machlus KR, Martínez-Bonet M, Lee PY, Wactor A, Nelson-Maney N, Morris A, Guo L, Weyrich A, Sola-Visner M, Boilard E, Italiano JE, Nigrovic PA (2019) Megakaryocyte emperipolesis mediates membrane transfer from intracytoplasmic neutrophils to platelets. Elife 8:e44031. https://doi.org/10.7554/eLife.44031
47. Sun Y, Wu B, Yan S, Zhang J, Zhang R, Zhu S (2013) Preparation of hemostatic sponge used for dressing, involves preparing chitosan aqueous solution, injecting into mold, freezing chitosan aqueous solution in mold, freeze-drying frozen material and post-processing chitosan sponge. CN103028135-A, 2013–N96850
48. Kim C, Lee S, Lim J, Son Y, Kim K, Gin Y, Kim CH, Lee SJ, Lim IJ, Son YS (2017) Method of producing a porous chitosan scaffold comprises freeze-drying of an aqueous acidic solution having chitosan and a solvent, and neutralizing the aqueous acidic solution. WO2007111416-A1
49. Lafantaisie-Favreau C-H, Guzmán-Morales J, Sun J, Chen G, Harris A, Smith TD, Carli A, Henderson J, Stanish WD, Hoemann CD (2013) Subchondral pre-solidified chitosan/blood implants elicit reproducible early osteochondral wound-repair responses including neutrophil and stromal cell chemotaxis, bone resorption and repair, enhanced repair tissue integration and delayed matrix deposition. BMC Musculoskelet Disord 14:27. https://doi.org/10.1186/1471-2474-14-27
50. Ghazi Zadeh L, Chevrier A, Lamontagne M, Buschmann MD, Hoemann CD, Lavertu M (2019) Multiple platelet-rich plasma preparations can solubilize freeze-dried chitosan formulations to form injectable implants for orthopedic indications. Biomed Mater Eng 30:349–364. https://doi.org/10.3233/BME-191058
51. Benesch J, Tengvall P (2002) Blood protein adsorption onto chitosan. Biomaterials 23:2561–2568. https://doi.org/10.1016/S0142-9612(01)00391-X
52. Rao SB, Sharma CP (1997) Use of chitosan as a biomaterial: studies on its safety and hemostatic potential. J Biomed Mater Res 34:21–28
53. Hoemann CD, Hurtig M, Rossomacha E, Sun J, Chevrier A, Shive MS, Buschmann MD (2005) Chitosan-glycerol phosphate/blood implants improve hyaline cartilage repair in ovine microfracture defects. The Journal of Bone & Joint Surgery 87:2671–2686. https://doi.org/10.2106/JBJS.D.02536
54. del Conde I, Crúz MA, Zhang H, López JA, Afshar-Kharghan V (2005) Platelet activation leads to activation and propagation of the complement system. J Exp Med 201:871–879. https://doi.org/10.1084/jem.20041497
55. Uchimido R, Schmidt EP, Shapiro NI (2019) The glycocalyx: a novel diagnostic and therapeutic target in sepsis. Crit Care 23:16. https://doi.org/10.1186/s13054-018-2292-6
56. Ellies LG, Ditto D, Levy GG, Wahrenbrock M, Ginsburg D, Varki A, Le DT, Marth JD (2002) Sialyltransferase ST3Gal-IV operates as a dominant modifier of hemostasis by concealing asialoglycoprotein receptor ligands. Proc Natl Acad Sci U S A 99:10042–10047. https://doi.org/10.1073/pnas.142005099
57. Grewal PK, Uchiyama S, Ditto D, Varki N, Le DT, Nizet V, Marth JD (2008) The Ashwell receptor mitigates the lethal coagulopathy of sepsis. Nat Med 14:648–655. https://doi.org/10.1038/nm1760
58. Dang CV, Shin CK, Bell WR, Nagaswami C, Weisel JW (1989) Fibrinogen sialic acid residues are low affinity calcium-binding sites that influence fibrin assembly. J Biol Chem 264:15104–15108. https://doi.org/10.1016/S0021-9258(18)63817-7
59. Varki A, Schauer R (2009) Sialic acids. In: Varki A, Cummings RD, Esko JD, Freeze HH, Stanley P, Bertozzi CR, Hart GW, Etzler ME Essentials of glycobiology. 2nd edn. Cold Spring Harbor Laboratory Press, Cold Spring Harbor, http://www.ncbi.nlm.nih.gov/books/NBK1920/. Accessed 20 Mar 2021
60. Malette WG, Quigley HJ, Gaines RD, Johnson ND, Rainer WG (1983) Chitosan: a new hemostatic. Ann Thorac Surg 36:55–58. https://doi.org/10.1016/s0003-4975(10)60649-2

61. Klokkevold PR, Lew DS, Ellis DG, Bertolami CN (1991) Effect of chitosan on lingual hemostasis in rabbits. J Oral Maxillofac Surg 49:858–863. https://doi.org/10.1016/0278-2391(91)90017-G
62. Chou T-C, Fu E, Wu C-J, Yeh J-H (2003) Chitosan enhances platelet adhesion and aggregation. Biochem Biophys Res Commun 302:480–483. https://doi.org/10.1016/S0006-291X(03)00173-6
63. Okamoto Y, Yano R, Miyatake K, Tomohiro I, Shigemasa Y, Minami S (2003) Effects of chitin and chitosan on blood coagulation. Carbohydr Polym 53:337–342. https://doi.org/10.1016/S0144-8617(03)00076-6
64. Lin C-W, Lin J-C (2003) Characterization and blood coagulation evaluation of the water-soluble Chitooligosaccharides prepared by a facile fractionation method. Biomacromolecules 4:1691–1697. https://doi.org/10.1021/bm034129n
65. Hattori H, Ishihara M (2015) Changes in blood aggregation with differences in molecular weight and degree of deacetylation of chitosan. Biomed Mater 10:015014. https://doi.org/10.1088/1748-6041/10/1/015014
66. Whang HS, Kirsch W, Zhu YH, Yang CZ, Hudson SM (2005) Hemostatic agents derived from chitin and chitosan. J Macromol Sci C 45:309–323. https://doi.org/10.1080/15321790500304122
67. Behrens AM, Sikorski MJ, Kofinas P (2014) Hemostatic strategies for traumatic and surgical bleeding: hemostatic strategies for traumatic and surgical bleeding. J Biomed Mater Res 102:4182–4194. https://doi.org/10.1002/jbm.a.35052
68. Romani AA, Ippolito L, Riccardi F, Pipitone S, Morganti M, Baroni MC, Borghetti AF, Bettini R (2013) In vitro blood compatibility of novel hydrophilic chitosan films for vessel regeneration and repair. Adv Biomater Sci Biomed Appl. https://doi.org/10.5772/52706
69. Sundaram MN, Mony U, Varma PK, Rangasamy J (2021) Vasoconstrictor and coagulation activator entrapped chitosan based composite hydrogel for rapid bleeding control. Carbohydr Polym 258:117634. https://doi.org/10.1016/j.carbpol.2021.117634
70. Marchand C, Rivard G-E, Sun J, Hoemann CD (2009) Solidification mechanisms of chitosan–glycerol phosphate/blood implant for articular cartilage repair. Osteoarthr Cartil 17:953–960. https://doi.org/10.1016/j.joca.2008.12.002
71. Hoemann CD, Chen G, Marchand C, Tran-Khanh N, Thibault M, Chevrier A, Sun J, Shive MS, Fernandes MJG, Poubelle PE, Centola M, El-Gabalawy H (2010) Scaffold-guided subchondral bone repair: implication of neutrophils and alternatively activated Arginase-1+ macrophages. Am J Sports Med 38:1845–1856. https://doi.org/10.1177/0363546510369547
72. Bell AD, Hurtig MB, Quenneville E, Rivard G-É, Hoemann CD (2017) Effect of a rapidly degrading Presolidified 10 kDa chitosan/blood implant and subchondral marrow stimulation surgical approach on cartilage resurfacing in a sheep model. Cartilage 8:417–431. https://doi.org/10.1177/1947603516676872
73. Guzmán-Morales J, Lafantaisie-Favreau C-H, Chen G, Hoemann CD (2014) Subchondral chitosan/blood implant-guided bone plate resorption and woven bone repair is coupled to hyaline cartilage regeneration from microdrill holes in aged rabbit knees. Osteoarthr Cartil 22:323–333. https://doi.org/10.1016/j.joca.2013.12.011
74. Dwivedi G, Chevrier A, Hoemann CD, Buschmann MD (2019) Injectable freeze-dried chitosan-platelet-rich-plasma implants improve marrow-stimulated cartilage repair in a chronic-defect rabbit model. J Tissue Eng Regen Med 13:599–611. https://doi.org/10.1002/term.2814
75. Zhao X, Guo B, Wu H, Liang Y, Ma PX (2018) Injectable antibacterial conductive nanocomposite cryogels with rapid shape recovery for noncompressible hemorrhage and wound healing. Nat Commun 9:2784. https://doi.org/10.1038/s41467-018-04998-9
76. Ghavidel Mehr N, Hoemann CD, Favis BD (2015) Chitosan surface modification of fully interconnected 3D porous poly(ε-caprolactone) by the LbL approach. Polymer 64:112–121. https://doi.org/10.1016/j.polymer.2015.03.025

77. Mao C, Qiu Y, Sang H, Mei H, Zhu A, Shen J, Lin S (2004) Various approaches to modify biomaterial surfaces for improving hemocompatibility. Adv Colloid Interface Sci 110:5–17. https://doi.org/10.1016/j.cis.2004.02.001
78. Yatomi Y, Igarashi Y, Yang L, Hisano N, Qi R, Asazuma N, Satoh K, Ozaki Y, Kume S (1997) Sphingosine 1-phosphate, a bioactive sphingolipid abundantly stored in platelets, is a Normal constituent of human plasma and serum. J Biochem 121:969–973. https://doi.org/10.1093/oxfordjournals.jbchem.a021681
79. Jeon J-H, Kim Y-S, Choi E-J, Cheon S, Kim S, Kim J-S, Jang JS, Ha WS, Park ST, Park CS, Park K, Park B-K (2001) Implication of co-measured platelet factor 4 in the reliability of the results of the plasma transforming growth factor-β1 measurement. Cytokine 16:102–105. https://doi.org/10.1006/cyto.2001.0895
80. Erbel C, Korosoglou G, Ler P, Akhavanpoor M, Domschke G, Linden F, Doesch AO, Buss SJ, Giannitsis E, Katus HA, Gleissner CA (2015) CXCL4 plasma levels are not associated with the extent of coronary artery disease or with coronary plaque morphology. PLoS One 10:e0141693. https://doi.org/10.1371/journal.pone.0141693
81. Du Q, Li E, Liu Y, Xie W, Huang C, Song J, Zhang W, Zheng Y, Wang H, Wang Q (2018) CTAPIII/CXCL7: a novel biomarker for early diagnosis of lung cancer. Cancer Med 7:325–335. https://doi.org/10.1002/cam4.1292
82. Franciotta D, Zardini E, Ravaglia S, Piccolo G, Andreoni L, Bergamaschi R, Romani A, Tavazzi E, Naldi P, Ceroni M, Marchioni E (2006) Cytokines and chemokines in cerebrospinal fluid and serum of adult patients with acute disseminated encephalomyelitis. J Neurol Sci 247:202–207. https://doi.org/10.1016/j.jns.2006.05.049
83. Neubauer H, Petrak F, Zahn D, Pepinghege F, Hägele A-K, Pirkl P-A, Uhl I, Juckel G, Mügge A, Herpertz S (2013) Newly diagnosed depression is associated with increased beta-thromboglobulin levels and increased expression of platelet activation markers and platelet derived CD40-CD40L. J Psychiatr Res 47:865–871. https://doi.org/10.1016/j.jpsychires.2013.03.011
84. Roberts HR, Monroe DM III, Hoffman M (2001) Molecular biology and biochemistry of the coagulation factors and pathways of hemostasis. In: Williams hematology. 6th edn. McGraw-Hill, New York, pp 1409–1434
85. Butenas S, Mann KG (2002) Blood coagulation. Biochemistry (Mosc) 67:3–12. https://doi.org/10.1023/a:1013985911759
86. Miller CH, Haff E, Platt SJ, Rawlins P, Drews CD, Dilley AB, Evatt B (2003) Measurement of von Willebrand factor activity: relative effects of ABO blood type and race. J Thromb Haemost 1:2191–2197. https://doi.org/10.1046/j.1538-7836.2003.00367.x
87. Ruiz FA, Lea CR, Oldfield E, Docampo R (2004) Human platelet dense granules contain polyphosphate and are similar to Acidocalcisomes of bacteria and unicellular eukaryotes. J Biol Chem 279:44250–44257. https://doi.org/10.1074/jbc.M406261200
88. Klemm KM, Klein MJ (2017) Biochemical markers of bone metabolism (chapter 15). In: Henry's clinical diagnosis and management by laboratory methods. 23rd edn. Elsevier, St Louis, pp 188–204